

Spreading height and critical conditions for the collapse of turbulent fountains in stratified media

L. G. Sarasua, D. Freire, C. Cabeza, Arturo C. Marti

Instituto de Física, Facultad de Ciencias, Universidad de la República, Iguá 4225, Montevideo, Uruguay

Axisymmetric fountains in stratified environments rise until reaching a maximum height, where the vertical momentum vanishes, and then falls and spread radially as an annular plume following a well-known top-hat profile. Here, firstly, we generalize the model of Morton et al. (Proc. R. Soc. Lond. A **234**, 1, 1956), in order to correctly determine the dependence of the maximum height and the spreading height with the parameters involved. We obtain the critical conditions for the collapse of the fountain, *i.e.* when the jet falls up to the source level, and show that the spreading height must be expressed as a function of at least two parameters. To improve the quantitative agreement with the experiments we modify the criterion to take the mixing process in the down flow into account. Numerical simulations were implemented to estimate the parameter values that characterizes this merging. We show that our generalized model agrees very well with the experimental measurements.

I. INTRODUCTION

A fountain is a vertical buoyant jet in which the buoyancy force and the jet initial velocity act in opposite directions. If the buoyancy force acts in the same direction of the jet velocity it is said the flow is a plume. Fountains and plumes are encountered frequently in nature and technical applications such as selective withdrawal, desalination plants, and the replenishment of magma chambers. Since the dynamical behavior of fluids within stratified media presents a problem of considerable interest across a number of fields, turbulent fountains and plumes in uniform and stratified mediums have been the subject of investigation for decades [1–14].

The dynamics of the fountain in a stratified medium can be schematized as follows. At an initial stage the fountain decelerates due to both the entrainment of ambient fluid and the negative buoyancy force, and it reaches a maximum height where the momentum is zero. Then the flow reverses direction and falls as an annular plume around the fountain core. Depending on the initial fluxes of momentum and buoyancy and the stratification profile, the fountain spreads outwards at a non zero spreading height above the source level or the flow totally collapses, *i.e.* falls to the level of the source.

The theoretical description of turbulent fountains in the quasi-steady regime can be done on the basis of the influential work of Morton, Taylor and Turner [15–17], who derived equations (so called *MTT* equations) for the evolution of volume, momentum, and buoyancy fluxes in fountains. In deriving these equations, it is assumed that the horizontal velocity at which the ambient fluid enters into the fountain is proportional to the vertical velocity in the fountain, with a proportionality constant α called entrainment coefficient. Although successful in predicting the evolution in a uniform ambient or the maximum height in plumes [2], the *MTT* equations do not describe the dynamics after the vertical velocity reverses its direction.

Bloomfield and Kerr proposed that the spreading height, z_s , can be obtained matching to the height where

the fluid of the environment has the density of the fluid at the maximum height, z_m , and used this condition to obtain estimations of z_m and z_s combining different models [6]. This may be considered as a first estimation because the mentioned condition does not take into account the mixing between the jet and ambient fluids in the down-flow that occurs after the fountain reverses direction. In a later work Bloomfield and Kerr developed a theoretical model to predict the maximal spreading height [18] based on the equations derived by McDougall for an axisymmetric fountain in an homogeneous fluid [19]. In this model the authors assumed entrainment equations which depends on three entrainment constants.

A while later, Kaminski et al. [20], developed an expression for the entrainment parameter α depending on three parameters that can be determined using the experimental data. A comparison between the predictions based on this expression and the experimental data were given in [21] for the case of homogeneous mediums. Mehaddi et. al. [22] conducted a study of fountains in stratified environments and obtained expression for the maximum height, although the spreading behavior of the fountain was not considered in this investigation. Papanicolau et al. conducted an experimental study on the collapse and spreading of turbulent fountains and performed a comparison with those obtained in [6]. As it has been pointed out by various authors [23, 25, 26], to assume a constant α is an approximation because the entrainment coefficient depends on the turbulence intensity and as a consequence it can vary along the rise of the fountain.

In this work we study models for the rise and spreading of a fountain in a stratified medium. Although new equations are introduced in the models, a constant value of α is assumed. Our aim is to develop a model which is able to describe the dependence of z_m , z_s with the parameters that determine the flow and the critical conditions for the total collapse of the fountain. The work is organized as follows. In Sec. II we give an account of the *MTT* equations and discuss the capability of the top-hat version of these equations to determine the spreading level.

In Sec. III we present new equations to avoid a drawback detected in the Gaussian version of the *MTT* equations. In section IV we discuss a model which includes the top-hat and Gaussian models as particular cases and present the numerical results obtained with the different models. In section V our conclusions are summarized.

II. THE *MTT* ENTRAINMENT EQUATIONS

We begin considering the equations derived by Morton, Taylor and Turner [15, 17] in the Boussinesq approximation for top-hat axisymmetric steady fountains in a linearly stratified environment. In the model the fountain is characterized by an ambient fluid, initially quiescent, with density $\rho_0(z)$, being the density at the bottom $\rho_0(z=0) = \rho_{00}$. A relevant quantity is the buoyancy frequency N , defined as $N^2 = -(g/\rho_{00})(d\rho_0/dz)$. The vertical jet with radius $b(z)$ it is assumed to enter in that region with velocity u . The *MTT* model is usually written in terms of vertical flow of mass $W = b^2u$, the vertical flow of momentum $M = b^2u^2$ and buoyancy flux $F = b^2ug(\rho_0 - \rho)/\rho_{00}$. With these definitions, the model equations are

$$\frac{dW}{dz} = 2\alpha M^{1/2}, \quad \frac{dM^2}{dz} = 2FW, \quad \frac{dF}{dz} = -N^2W, \quad (1)$$

where g is the gravitational acceleration. This set of equations together with the condition according to which z_s is the height where the fluid of the environment has the density of the fluid at the maximum height

$$\rho(z_m) = \rho_0(z_s), \quad (2)$$

are sufficient to obtain values of z_m and z_s .

Although the derivation of the *MTT* equations is based on the assumptions that the flow is self-similar and the entrainment coefficient is constant, this model has been successfully used by Bloomfield and Kerr [6] to predict the maximal height z_m of the fountains. These authors used the condition (2) to obtain an estimation of the spreading height z_s . However, the approach followed in [6] has the inconvenience that it uses two different models to obtain z_m and z_s . While z_s is estimated by combining Eq.(2) and the integration of *MTT* equations with the initial condition $F = 0$ at the virtual source, z_m is obtained integrating (1) with the experimental source conditions.

We note that here z_m is the maximal height of the fountain in the steady regime. It should not be confused with the maximal height reached in the transitory stage. In this section we analyze the results that are obtained when the criterion given by Eq.(2) is used in combination with the integration of (1) and the same conditions at the source are imposed to determine z_m and z_s . Thus, these two heights will be determined using the same model.

A. Dimensionless equations

We consider now the dimensionless form of the governing equations (1) taking the radius of the source d and the velocity at the source U as the length and velocity scales respectively. Then we define the dimensionless variables $x = z/d$, $W = Wd^{-2}U^{-1}$, $M = Md^{-2}U^{-2}$, $F = Fd^{-1}U^{-3}$, $N = dU^{-1}N$. Thus, the dimensionless equations become

$$\frac{dW}{dx} = 2\alpha M^{1/2}, \quad \frac{dM^2}{dx} = 2FW, \quad \frac{dF}{dx} = -N^2W, \quad (3)$$

with the initial conditions at the source:

$$W = 1, \quad M = 1, \quad F = -\text{Fr}^{-2}, \quad (4)$$

where Fr is the Froude number defined as $\text{Fr} = U/\sqrt{gd(\rho(0) - \rho_{00})/\rho_{00}}$. As it follows from the equations (3) and initial conditions (4), the behavior of the flow is determined by the three independent dimensionless numbers N , Fr and α . This is related to the fact for the fountain in a linearly stratified medium three independent characteristic lengths can be defined:

$$\begin{aligned} l_Q &= W_i \alpha^{-1} M_i^{-1/2} \\ l_M &= M_i^{3/4} \alpha^{-1/2} F_i^{-1/2} \\ l_H &= F_i^{1/4} \alpha^{-1} N^{-3/4} \end{aligned} \quad (5)$$

where the subscript i refer to the values of M, W, F at the source [2]. In addition, the radius of the jet at the source is another relevant longitude. As a consequence, three independent dimensionless parameters can be constructed by dividing the lengths l_Q, l_M, l_H by d .

In [6], [18] Bloomfield and Kerr argued that the maximal and spreading heights are functions of the form

$$z_j = f_j(\sigma) M^{-3/4} F^{-1/2} \quad (6)$$

where $f_j(\sigma)$ are functions of only σ , defined as $\sigma = M^2 N^2 / F^2$, with $j = m, s$. We notice that this expression does not include the dependence on α . Owing to the fact that α is related to the turbulent mixing, it is a function of the Reynolds number $Re = Ud/\nu$. Thus, the no dependence of equation (6) with Re is a serious limitation. In addition, the coefficient α appears in the dimensionless parameters (5) that define the flow. As a consequence, we expect that α must appear in the expression of z_s . In the present work we shall consider the dependence of the maximal and the spreading heights on all the relevant parameters that determine the flow.

Although the flows are determined by the three independent dimensionless numbers α, N and Fr , the number of relevant parameters may be reduced by defining the function $H = F/\alpha$ and $x = \alpha x$. In this case, the Eqs.(3) become

$$\frac{dW}{dx} = 2M^{1/2}, \quad \frac{dM^2}{dx} = 2HW, \quad \frac{dH}{dx} = -\beta^2 W, \quad (7)$$

where $\beta = N/\alpha$. The initial conditions at the source are now

$$W = 1, M = 1, H = \eta^{-1}, \quad (8)$$

where $\eta = \alpha Fr^2$. From the equations (7), it can be seen that finally the dimensionless flow only depends on the two dimensionless parameters η and β . This is a very useful simplification, because it implies that the fountain regimes can be represented in a two dimensional diagram.

As already mentioned, the dimensionless spreading height $h_s = z_s/d$ will be obtained as a first approximation using the condition (2). With this purpose we write such relation in terms of the dimensionless variables. From (2) it follows that $(\rho(h_m) - \rho_0(h_m)) + (\rho_0(h_m) - \rho_0) = (\rho_0(h_s) - \rho_0)$, which can be written as $(\rho(h_m) - \rho_0(h_m)) + h_m d\rho/dz = h_s d\rho_0/dz$. Using the definitions of F and Q we obtain the value of h_s as a function of the dimensionless maximum height $h_m = z_m/d$:

$$h_s = h_m + F'(h_m)Q'(h_m)^{-1}N'^{-2}. \quad (9)$$

B. Numerical results

In Fig. 1 the values of h_m and h_s are shown, which were obtained integrating the Eqs. (7), (9) with the boundary conditions (8). It can be seen that the dependence of h_m, h_s with σ are in accordance with the experimental data [6]. For values of σ below a critical value σ_c , h_s goes to zero which means that the fountain collapsed. We note that the variation of h_s with σ is very abrupt near the collapse at $\sigma = \sigma_c$. This is in agreement with the experimental data [6, 24]. In Fig. 2 the functions H, F, W are shown, as a function of x for the case $N = 0.05, Fr = 16$. The curves of Fig. 1 correspond to $\eta = 20$. For other values of η , the curves are similar but the value of σ_c changes, as it is plot in Fig. 3. These results contradict the hypothesis (6), according to which h_s is determined by a function that is proportional to a function that only depends on σ . Following this relation, the critical condition $z_s = 0$ is given by $f_j(\sigma) = 0$ (Eq.(6)), which would determine a unique value of σ_c , independent on Fr , or η . The results plot in Fig. 3 show that this is not correct.

We also tested the relation (6) in another way. According to this relation, $z_m = f_m(\sigma)M^{-3/4}F^{-1/2}$, which can be written as $h_m Fr^{-1} = f_m(\sigma)$. This means that $h_m Fr^{-1}$ should has a unique value for a given value of σ . In Fig. 4 curves of $h_m Fr^{-1}$ are shown and it can be seen that they do not overlap. It could be argued that the approximations performed to obtain the equations (7) could explain the differences with the predictions of Eq. (6). However, this is not the case. The drawback in deriving the Eq. (6) is to assume that h_m, h_s can be written in terms of the length scale for an homogeneous environment [6] and σ , without including α explicitly.

In Fig. 5 the critical value for the collapse of the fountain as a function of η is shown. For this curve

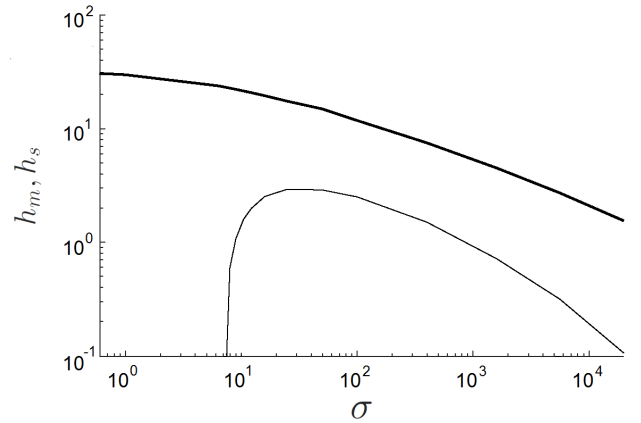


FIG. 1. Maximum (thick line) and spreading (thin line) dimensionless heights h_m, h_s as a function of σ for $\eta = 20$. The collapse of the fountain occurs in this case for $\sigma_c = 6.89$.

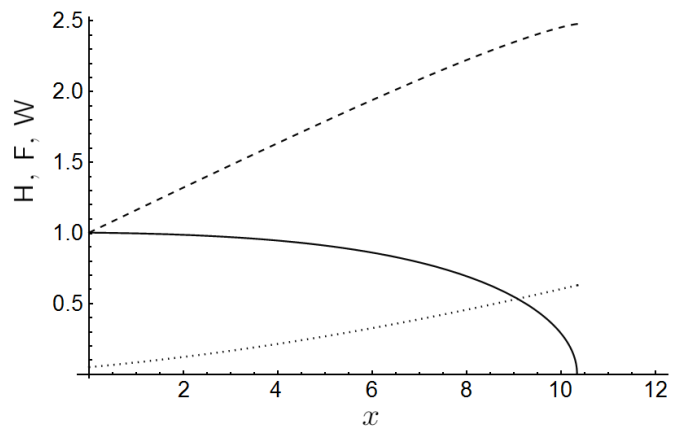


FIG. 2. Plot of the functions M (solid line), W (dashed line) and $-H$ (dotted line) as a function of x , for $N = 0.05, Fr = 16$.

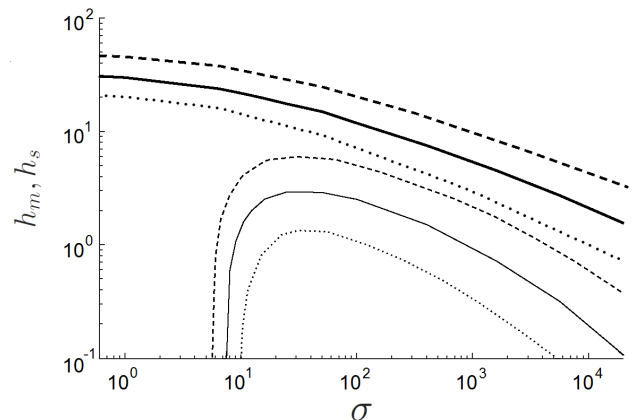


FIG. 3. Dimensionless maximal height h_m (thick lines) and spreading height h_s (thin lines) as a function of σ for $\eta = 40$ (dashed), 20 (solid) and 10 (dotted line). From the figure the changes of σ_c under variations of η are shown.

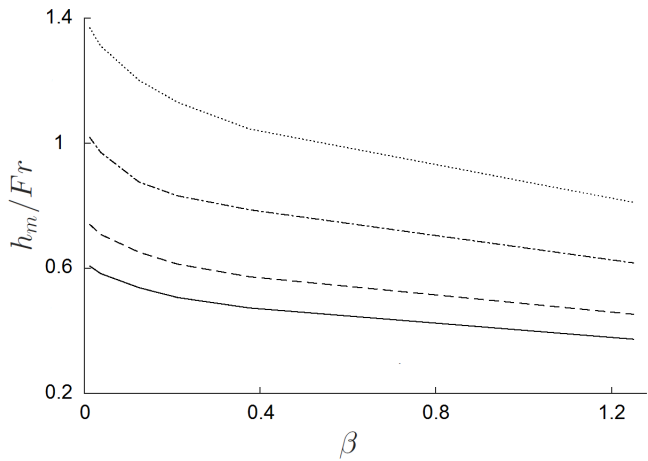


FIG. 4. Values of h_m/Fr , for $\sigma = 25$ (solid line), 100 (dashed), 400 (dashdotted) and 900 (dotted).

it can be seen that the modification of α can induce a change for the collapse to the buoyant situation. Since $\sigma = M^2 N^2 / Fr^2$ is independent of α , an increment of $\eta = \alpha Fr^2$ due to an increment of α maintaining fixed Fr can produce a transition from the fountain collapse to the fountain spreading above the source (buoyant regime). Although the typical values of the entrainment coefficient α are around 0.08 for top-hat profiles and 0.06 for Gaussian profiles [3, 6], there has been a significant variation in the values of α obtained in distinct experiments [20, 26]. This has been attributed to differences in the experimental setup and source conditions [26]. Freire et al. [27, 28] showed that the value of α can be modified artificially by the introduction of fluctuations. In this work it has been observed that z_m and thus α can be modified by the use of meshes at the source, keeping constant the other parameters that determine the flow. This shows that in certain cases the collapse can be controlled and avoided by the introduction of fluctuations, which is an interesting fact from the point of view of practical applications.

In the Fig. 6 the regions for the collapse or no collapse of the fountain as a function of $\beta = N'/\alpha$ and $\eta = \alpha Fr^2$ are shown. In this figure the curves for constant spreading height h_s are also plotted. In Fig. 7 the values of h_m and h_s as a function of σ at a constant value of β are shown.

C. Mixing approximation in the downflow

As already mentioned, the model considered up to now describes in correct form the dependence of the fountain flow on the relevant parameters at a qualitative level, but it does not include the mixing that takes place after the fountain reversed the velocity direction. As a consequence, there are important numerical differences between the critical values predicted by the model and those

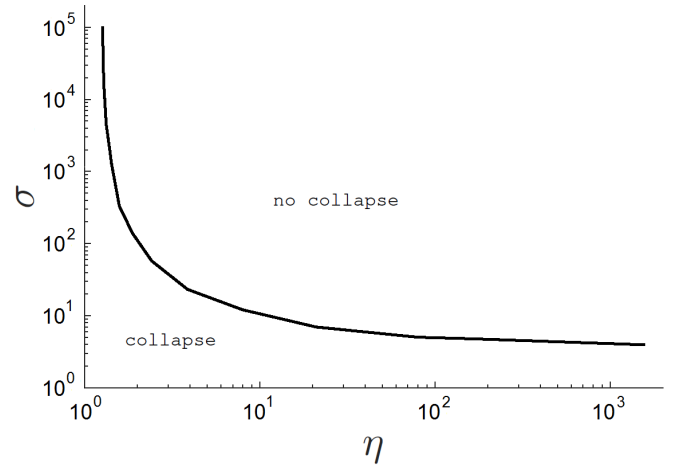


FIG. 5. Critical values of σ for the collapse of the fountain in the top-hat model, using the condition (2). For values of σ above the critical line, the fountain spreads laterally above the source level.

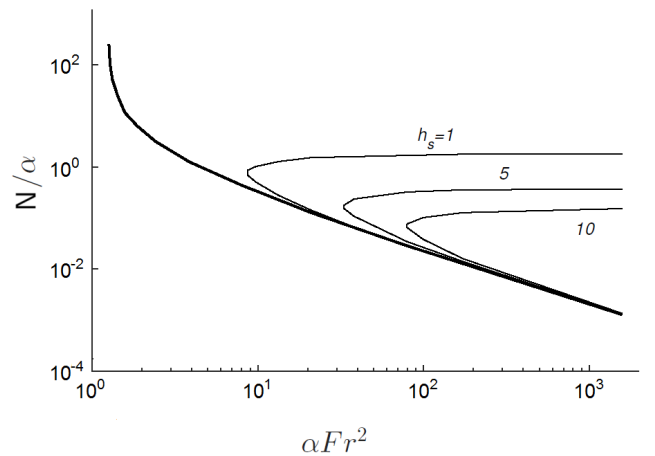


FIG. 6. Same as in Fig. 5 but in function of Fr , α and N . Above the critical line (thick line) there is no collapse of the fountain. In the figure the curves of constant spreading height h_s are also shown, corresponding to values indicated on the curves. When the mixing in the downflow is considered, these curves are modified.

observed experimentally. In order to include these second merging effect, we shall define a parameter γ that represents the proportion of environment fluid to jet fluid that mixes to form the fountain fluid at the spreading region. As a consequence, the criterion (2) must be modified in the form:

$$(1 - \gamma)\rho(z_m) + \frac{\gamma}{2}(\rho_0(z_m) + \rho_0(z_s)) = \rho_0(z_s). \quad (10)$$

Here $(\rho_0(z_m) + \rho_0(z_s))/2$ is an average of the environment density in the region around the downflow and $0 \leq \gamma < 1$. From the above expression we obtain that $\rho_0(h_m) - \rho(h_m) = ((1 - \gamma/2)/(1 - \gamma))(\rho_0(h_m) - \rho_0(h_s))$. Operating in similar form that has been done to derive

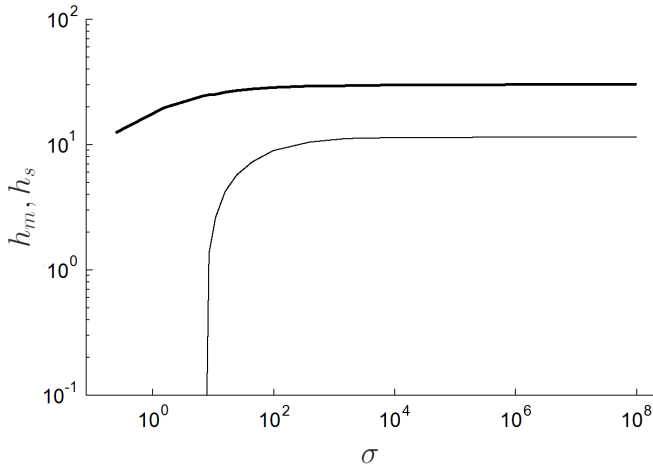


FIG. 7. Values of h_m (thick line) and h_s (thin line) as a function of σ at constant $\beta = 0.125$.

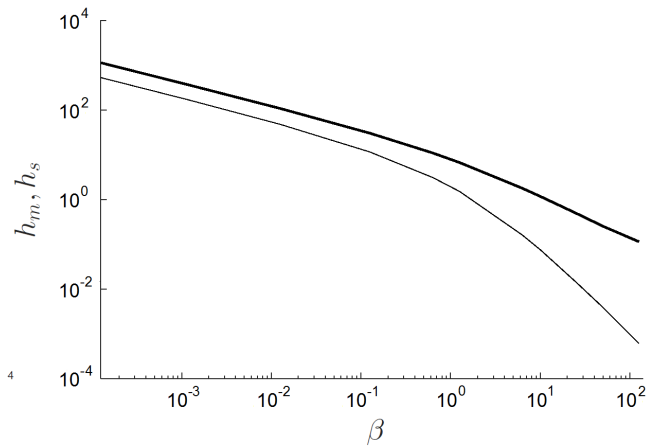


FIG. 8. Values of h_m (thick line) and h_s (thin line) as a function of β for zero buoyancy flux ($\eta \rightarrow \infty$). There is no collapse under this condition.

(9), we obtain that

$$h_s = h_m + 2 \left(\frac{1-\gamma}{2-\gamma} \right) F(h_m) Q(h_m)^{-1} N^{-2}. \quad (11)$$

In Fig. 9 the critical values σ_c obtained with the top-hat model and the condition (11) using $\gamma = 0.25$ are shown. In the figure the values of σ_c of for $\gamma = 0$ are also included, which correspond to the original condition (2). As it can be seen, the mixture in the downflow reduces the value of σ_c , increasing the region for which there is no collapse of the fountain. This is caused by the fact that the mixing reduces the density of the fountain, favoring its buoyancy. This effect is more pronounced for small values of η .

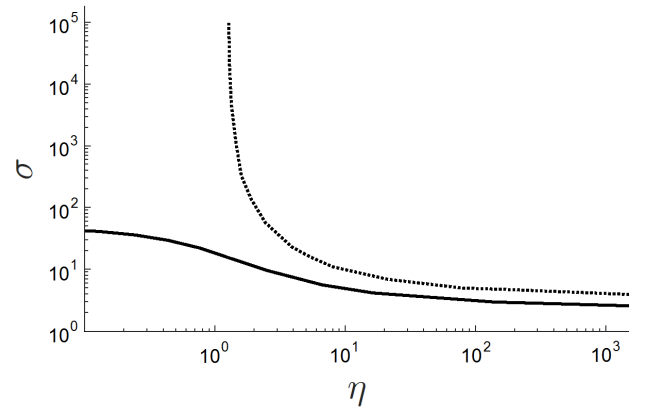


FIG. 9. Critical values of σ for the collapse of the fountain with top-hat profile obtained with the modified condition (11) and $\gamma = 0.25$ (solid line) to include the mixing in the downflow. In the plot it is also included the critical line for which $\gamma = 0$ (dotted line).

III. GAUSSIAN FOUNTAINS

In the case of Gaussian fountains, the *MTT* equations are:

$$\frac{dW}{dz} = 2\alpha M^{1/2}, \quad \frac{dM^2}{dz} = 4FW, \quad \frac{dF}{dz} = -2N^2W \quad (12)$$

[15]. By integration of these equations and the use of criteria (2), values of h_s were obtained for the case of zero buoyancy flux $\text{Fr}^{-1} = 0$ ($\eta \rightarrow \infty$), which means that the density of the fountain equals the environment density at the source. Under these conditions the obtained values of the spreading heights were always negative. Since it is an experimental evidence that under the condition of zero buoyancy flux the fountains exhibit always positive values of h_s , it follows that the results given by the model are qualitatively wrong.

In order to visualize the cause of this non expected result we obtain the value of the fluid density in the jet. From the definition of F , it follows that

$$\Delta\rho^* = -\frac{F}{W} - N^2x \quad (13)$$

where $\Delta\rho^* = (gd/U)(\rho - \rho_{00})/\rho_{00}$ is a dimensionless measure of the fluid density inside the jet. In Fig. 10 the variation of $\Delta\rho^*$ with x for $N = 0.01$ and $\alpha = 0.06$ is shown. As it can be seen from this figure, the value of ρ increases with the height in all the considered cases for $\text{Fr}^{-1} = 0$, which is an unexpected behavior and explains why the values of h_s are negative. When the value of ρ at h_m is larger than ρ_{00} , the zero buoyancy level would be located below the source. When $\text{Fr}^{-1} > 0$, the situation is even worse since the values of h_s are smaller. This shows that Eqs.(12) predict an evolution of ρ which is not in accordance with the experimental observations.

Due to this failure of the model, in the next section we develop a different equation to describe the changes of ρ caused by the entrainment process.

A. Density equation

With the aim to avoid the mentioned drawback of the Gaussian model described by Eqs. (12), we developed a new equation to describe the evolution of the fluid density ρ . We assume that in the entrainment process, a mass m with volume V is mixed with a mass $\delta m'$ with volume $\delta V'$. Then the final density will be $\rho_f = (m + \delta m')/(V + \delta V')$. Assuming $\delta m' \ll m$, $\delta V' \ll V$, then we can write the variation of density as

$$\Delta\rho = \rho_f - \rho_i = (\rho' - \rho_i) \frac{\rho_i \delta m'}{\rho' m} \quad (14)$$

where $\rho_i = m/V$, $\rho' = \delta m'/\delta V'$. In the case of the Gaussian jet, the vertical velocity \tilde{u} and the density $\tilde{\rho}$ are assumed to be functions of the cylindrical coordinates (z, r) [15], with

$$\tilde{u}(z, r) = u(z)e^{-r^2/b^2} \quad (15)$$

and

$$\tilde{\rho}(z, r) = (\rho(z) - \rho_0)e^{-r^2/b^2} + \rho_0. \quad (16)$$

As a consequence of the forms of \tilde{u} and $\tilde{\rho}$ there is not a precise limit between the core and the outer region of the jet. In this case, an effective radius can be defined [15]. We shall adopt that the effective radius of the fountain is $R = b$. Then considering a vertical cylinder of height dz whose circular base coincides with the cross section of the jet of radius b , the mass that enters in such cylinder through its base during the time interval dt is

$$m = \int_0^b \tilde{\rho}(z, r) \tilde{u}(r, z) 2\pi r dr dt.$$

Substituting in the above expression (15) and (16), and performing simplification as $\int_0^1 \exp(-2x^2) x dx \approx 0.316$, we obtain that

$$m = 2\pi u b^2 (0.216(\rho - \rho_0) + 0.316\rho_0) dt. \quad (17)$$

On the other hand, the mass that enters through the lateral area is [15]

$$\delta m' = 2\pi \rho_0 b \alpha u dz dt. \quad (18)$$

The density ρ_i appearing in (14) is $\rho_i = m/V = V^{-1} \int_0^b \tilde{\rho}(r, z) 2\pi r dr dz$, where $V = \pi b^2 dz$ is the volume of the cylinder. Substituting (16) in the above expression and performing the already mentioned approximations in the definite integrals we obtain

$$\rho_i = 0.632(\rho - \rho_0) + \rho_0 \quad (19)$$

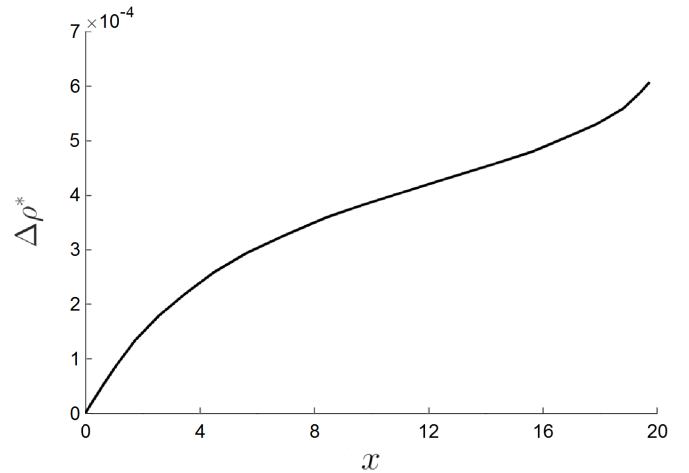


FIG. 10. Variation of the jet density ρ with the dimensionless height x obtained with de *MTT* equations for the Gaussian profile, with $N = 0.01$, $\alpha = 0.06$, $Fr^{-1} = 0$.

As in the original work of Morton et al. [15] we consider that the density variations are small in comparison to ρ_0 , $(\rho - \rho_0) \ll \rho_0$. Thus, using this approximation and substituting the expressions (17),(18),(19) in (14), identifying $\rho' = \rho_0$, $\Delta\rho = \rho(z + dz) - \rho(z)$, it is obtained that $d\rho = 0.835(\rho_0 - \rho) \frac{\alpha}{5} dz$, which can be written as

$$\frac{d\rho}{dz} = 0.835(\rho_0 - \rho) \alpha \frac{M^{1/2}}{W} \quad (20)$$

Defining $G = g(\rho - \rho_0)/\rho_{00}$, Eq.(20) can be expressed as:

$$\frac{dG}{dz} = -0.835\alpha W^{-1} M^{1/2} G + N^2. \quad (21)$$

The above equation and the two first equations of (1) are the governing equations of our model with Gaussian profile.

We comment that in the case of the top-hat profile, from the equation (14) the new equation is obtained:

$$\frac{dG}{dx} = -2\alpha W^{-1} M^{1/2} G + N^2.$$

This equation was obtained using $\rho_f = \rho(z + dz)$, $\rho_i = \rho(z)$, $\rho' = \rho_0(z)$, again and operating in similar way as has been done in section A. In section IV B we consider the results of a top-hat model including this equation.

FIG. 11. Critical line for the collapse of the fountain in the Gaussian model described by Eqs. (22), (11), with $\gamma = 0$ (solid line) and $\gamma = 0.25$ (dotted line).

B. Non-dimensional equations

By defining $J = (d/\alpha U^2)G$, the non-dimensional equations of the Gaussian model can be written as:

$$\begin{aligned}\frac{dW}{dx} &= 2M^{1/2}, \\ \frac{dM^2}{dx} &= -4JW^2, \\ \frac{dJ}{dx} &= -0.835W^{-1}M^{1/2}J + \beta^2\end{aligned}\quad (22)$$

where we used that by definition $F = -\alpha WJ$. The initial conditions at the source are

$$W = 1, M = 1, J = \eta^{-1}. \quad (23)$$

From the equations (22),(23) it follows that also in the modified Gaussian model the fountain regime is determined by the parameters η and β .

We solved the Eqs. (7) with the initial conditions (23) to obtain the critical conditions for the collapse of the fountain with Gaussian profile. The resulting critical line is shown in Fig.11.

IV. TOP-HAT-GAUSSIAN MODEL

Although the *MTT* equations have been formulated for the cases of top-hat and Gaussian profiles, in real situations it is observed that in many cases the profiles are not purely top-hat nor Gaussian [31]. This fact motivates us to consider a model in which the velocity of the jet is a combination of these two types of flows. Then we assume that the velocity and density are

$$\begin{aligned}\tilde{u}(z, r) &= (Ae^{-r^2/b^2} + B(1 - \Theta(r - b)))u(z), \\ \tilde{\rho}(z, r) &= A((\rho(z) - \rho_0)e^{-r^2/b^2} + \rho_0) \\ &\quad + B(\rho + (\rho_0 - \rho)\Theta(r - b)).\end{aligned}\quad (24)$$

where $\Theta(x)$ is the Heaviside function, defined as $\Theta(x) = 0$ if $r < b$, $\Theta(x) = 1$ if $r \geq b$, and u is the characteristic velocity, which corresponds to the velocity of the jet at the axis. Thus, in the model $A + B = 1$. To characterize the flow we introduce the parameter $\delta = 1 - A$. Hence, if $\delta = 0$ the model reduces to the Gaussian profile and if $\delta = 1$ the top hat model is recovered. As done in [15], we integrated the equation of momentum conservation in an infinite section to eliminate the dependence with r . Assuming again the Boussinesq condition, it is obtained that

$$C_1 \frac{d}{dz}(\pi \rho b^2 u^2) = -gb^2(\rho - \rho_0) \quad (25)$$

where $C_1 = 0.5A^3 + 1.764A^2B + 3AB^2 + B^3$. Thus the resulting equation is similar to the original *MTT* equations, except for the factor C . Then, it follows that this equation can be written as

$$\frac{dM^2}{dz} = 2C^{-1}FW. \quad (26)$$

On the other hand, we obtained an equation similar to (21) for the mixed flow,

$$\frac{dG}{dz} = -D\alpha W^{-1}M^{1/2}G + N^2, \quad (27)$$

where $C_2 = (0.264A + B)/(0.316A + 0.5B)$. Since the accepted values of α are near 0.06 and 0.08 for the Gaussian and top-hat profiles respectively, we assume that in the model $\alpha = 0.06 + 0.02\delta$. This assures that the usual values are recovered in the limiting cases $\delta = 0$ (Gaussian) and $\delta = 1$ (top hat). Alternatively, the value of α could be considered to be a free parameter. Thus, the dimensionless equations of the model are

$$\begin{aligned}\frac{dW}{dx} &= 2M^{1/2}, \\ \frac{dM^2}{dx} &= -2C_1^{-1}JW^2, \\ \frac{dJ}{dx} &= -C_2W^{-1}M^{1/2}J + \beta^2,\end{aligned}\quad (28)$$

with the initial conditions

$$W = 1, M = 1, J = \eta^{-1}. \quad (29)$$

A. Numerical simulations

Numerical simulations were implemented to obtain an estimation of the value of the parameter γ that has been introduced to take into account the mixing in the down-flow and to test other predictions of the model. The simulations were performed with the program *caffa3d.MBRi*, which is an open-source code that implements the Finite Volume Method (FVM). This solver has been tested for accuracy in benchmark flows and it has been shown to have second-order accuracy in space and time. The code solves numerically three-dimensional incompressible flows using curvilinear meshes structured by blocks. For more information about the solver we refer to [32],[33]. To validate the computational scheme, we contrasted the results with the experimental data of Freire et. al [27]. These experiments were conducted in a prismatic container with lateral walls of 0.4 m in width and 1 m in height. The ambient fluid was water and the density stratification was established fixing a temperature of 40°C at the top and 15°C at the bottom. The fluid jet was injected upwards through a nozzle of 8 mm diameter. Differing degrees of turbulence level were generated in the experiments using a stainless-steel wire mesh placed at the inlet port. In the numerical implementation, the

generation of disturbances produced by the wire mesh was simulated by the inclusion of white noise in the velocity components of the jet at the inlet. The intensity of the noise was varied to obtain the best fit of experimental observations. A comparison of the numerical and experimental results is given in Fig. 12, showing a very good agreement. These simulations were done using a noise level of 20% of the velocity magnitude at the inlet. After the validation of the program, we performed simulations for the non-zero buoyancy flux case considering different values of the buoyancy frequency N in the range $0.1 - 0.4 \text{ s}^{-1}$. The inlet velocity U was kept fixed at 0.11 m/s and the jet temperature at the inlet was fixed at the value $T_J = 10^\circ\text{C}$. Using the results of the temperature field and Eq.(10) the values of γ of different runs were calculated. The average value of the obtained values is $\gamma = 0.011 \pm 0.003$. We also contrasted the model with the results of the simulation in another way. As it can be observed in Fig. 6, h_s experiments a maximum when β is varied at a fixed value of η . The results of the simulation concerning the value of h_s are plotted in Fig. 13, showing that the prediction of the model is confirmed by the numerical simulation.

B. Comparison with experimental data

In order to compare the results of the different models with the experimental measurements, we first consider the case of zero buoyancy ($\text{Fr} \rightarrow \infty$). For the sake of convenience, the maximal and spreading heights h_m , h_s will be normalized with the characteristic length

$$l_j = (\pi M_i)^{1/4} N^{-1/2}$$

used by Papanicolau et al. [24] to plot their experimental data and those reported by Bloomfield and Kerr [7]. We will also consider the ratios z_s/z_m . In their experimental study, Papanicolau et al. concluded that in the limit $\sigma \rightarrow \infty$, which is the zero-buoyancy limit, the ratio z_m/l_j tends to the same value $z_m/l_j \approx 3.6$. Bloomfield and Kerr reported a similar behavior but with a different value in the zero-buoyancy limit $z_m/l_j \approx 2.88$. Papanicolau et al. attributed these differences to probable errors in the experimental procedure of Bloomfield and Kerr. However, the results of the present models suggest that the explanation can be another. Since h_m , h_s do not obey to universal functions of σ as it was incorrectly assumed in [6], there is not a universal value of z_m/l_j . This value depends on other conditions under which the experiment is done, such as the value of β . In Table I, the values of z_m/l_j , h_s/h_m obtained with the models and in the experiments are shown.

The results shown in the table were obtained for $N = 0.01$, which is a value that is representative of the conditions of the experiments in [6]. As it can be seen, for the above mentioned condition the results are close to the data in [6]. In the case of the Gaussian model, to obtain values near the data a value of $\gamma = 0.5$ was used,

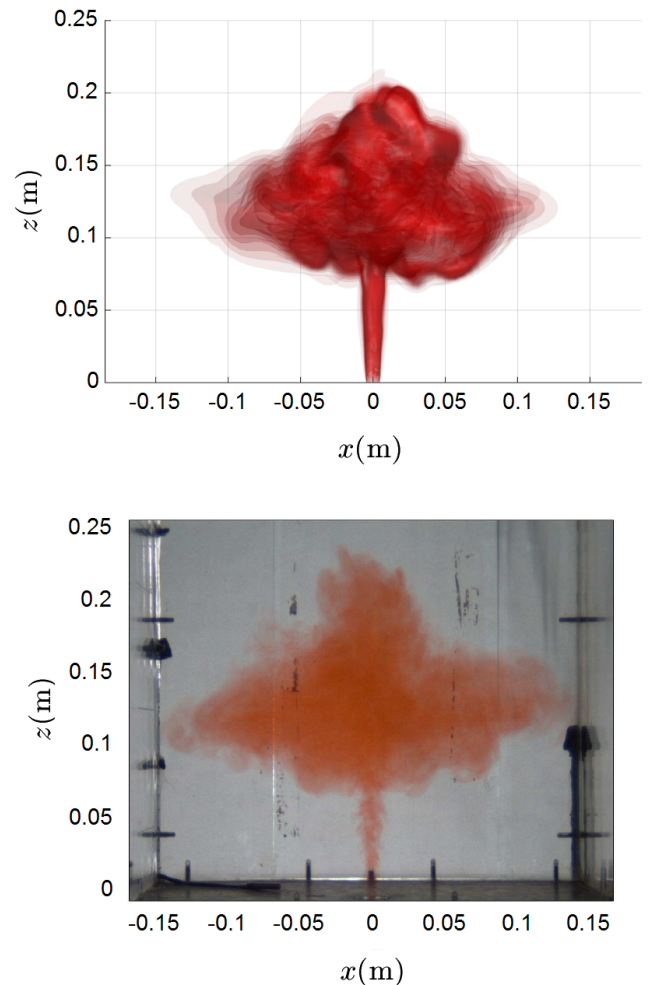


FIG. 12. Comparison between the experiments and simulations of the fountain spreading in the zero buoyancy case. The buoyancy frequency is $N = 0.23 \text{ s}^{-1}$, the radius of the nozzle $d = 4 \text{ mm}$ and the velocity at the inlet $U = 0.11 \text{ m/s}$.

TABLE I. Experimental data and results of the models for $N = 0.01$.

Study/model	z_m/l_j	z_s/l_j	z_s/z_m
Bloomfield and Kerr	2.88	1.35	0.47
Papanicolau et al.	3.58	1.94	0.54
Top-hat, $\gamma = 0.11$	2.25	0.93	0.41
Gaussian, $\gamma = 0.5$	1.96	0.89	0.45
Top-Hat-Gaussian, $\gamma = 0.18$, $\delta = 0.9$	2.26	0.98	0.43

which is probably not as realistic as it follows from the estimations that we did using the simulations. The best results were obtained with the mixed model with a flow that is closer to the top-hat profile than the Gaussian profile ($\delta = 0.9$). We note that the values of z_m/l_j , z_s/l_j are not universal but depend on β . The results in the table are closer to the data of [6] probably because we used

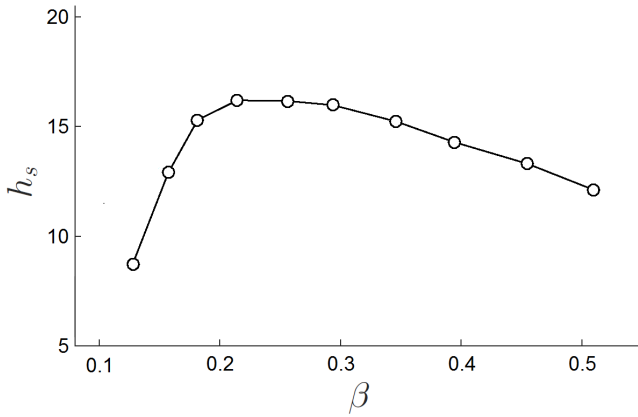


FIG. 13. Dimensionless height h_s as a function of β for $\eta = 8$ obtained with the numerical simulations in the nonzero buoyancy case. As it can be seen, h_s exhibits a maximum when it is plotted as a function of β at constant η , as it is predicted by the model.

a value of β that is in accordance with the conditions of these experiments.

We now consider the comparison between the critical values σ_c obtained in experiments performed with nonzero buoyancy flux at the source and those obtained with the model. In the experiments carried out by Bloomfield and Kerr, it was obtained that $\sigma_c \sim 5$ [7]. In this work the authors performed a series of experiments varying N and Fr , which implies that different values of η were covered. We estimate that a representative value of this parameter in such experiments is $\eta \sim 80$. Using the mixed models with $\delta = 0.9$, $\gamma = 0.18$ and $\eta = 80$ we obtained $\sigma_c = 4.6$ and $z_m/lj = 1.94$ at the critical point $\sigma = \sigma_c$, which are close to the values $\sigma_c = 5$, $z_m/lj \approx 2$ obtained in [7] (see also [24]).

V. CONCLUSION

In this work we considered models to describe the collapse or rise and spreading of axisymmetric turbulent fountains taking into account all the relevant parameters of the flow. In the first considered model we combine the *MTT* equations for the top-hat profile and the condition (2) to determine in a first approximation the dimensionless maximal and spreading heights h_m , h_s . In this model, all the fountain regimes can be specified by the two dimensionless parameters $\beta = N/\alpha$ and $\eta = \alpha Fr^2$. The results showed that the model describes in correct form at a qualitative level the dependence of h_m and h_s with all the parameters of the flow, including the conditions at the source and of the environment. We obtained the critical conditions to the collapse of the fountain, in

which case the flow does not become neutrally buoyant at a positive h_s , but falls to the source level. The dependence of h_s on σ is very abrupt around the collapse conditions, in accordance with the experimental data. The results showed that the relation $h_m = f(\sigma)M_0^{3/4}F_0^{-1/2}$ that has been proposed in various previous works [6, 7, 18] is not correct. The origin of the drawback is that this relation does not take into account all the dimensionless parameters determining the flow. This fact explains some important differences concerning the results of distinct experimental investigations [6],[24].

Although the predictions of the model concerning the dependence of h_m and h_s with the parameters controlling the phenomena are qualitatively correct, the numerical values do not fit the experimental data accurately. This discrepancy is caused by the fact that the model does not include the mixing that occurs between the falling flow and the environment after the jet attained the maximal height and reversed its direction. To correct this deficiency we modified the original condition used to estimate h_s to include the mixing in the downflow introducing a parameter γ . This modification increased the agreement between the predictions and the experimental data. The value of γ has been estimated by the use of numerical simulations. We also considered a model to describe jets with Gaussian profile. We showed that the classic *MTT* equations in the case of the Gaussian profile predict an incorrect evolution of the fluid density inside the jet, for which reason the spreading height obtained using Eqs.(1) and the condition (2) is always negative, which means that in this model the fountain collapses in all the cases. We derived a new equation to complete the description, which does not exhibit the problem described above. We show that the new set of equations together with Eq. (2) determine, from qualitative viewpoint, the dependence h_m and the h_s with σ correctly. In order to increase the quantitative quality of the model, we introduced a third model which assumes that the flow is a combination of a Gaussian and a top-hat jet. With this mixed model, very good agreements were obtained with the experimental data. Thus, we presented a model which captures in qualitative and quantitative form the dependence of the rise and spreading on all the fundamental parameters that characterizes the fountain. As a consequence, the mixed model can be used to predict the overall behavior of fountains in a stratified medium. Other predictions of the model were satisfactorily verified with the numerical simulations.

The authors would like to thank the Uruguayan institutions Programa de Desarrollo de las Ciencias Básicas (PEDECIBA), Agencia Nacional de Investigación e Innovación (ANII) and express their gratitude for the grant Física No lineal (ID 722) Programa Grupos I+D CSIC 2018 (Udelar, Uruguay).

-
- [1] A. W. Woods, Turbulent Plumes in Nature, *Annu. Rev. Fluid Mech.* **42** 391-412 (2010).
- [2] N. Kaye, Turbulent plumes in stratified environments: A review of recent work, *Atmos. Ocean*, **46**, 433-441 (2008).
- [3] G.R. Hunt and H.C. Burridge, Fountains in Industry and Nature, *Annu. Rev. Fluid Mech.* **47** 195-220 (2015).
- [4] J. S. Turner, Buoyant plumes and thermals, *Annu. Rev. Fluid Mech.* 1969 1 29-44
- [5] W. D. Baines, J. S. Turner and I. H. Campbell, Turbulent fountains in an open chamber, *J. Fluid Mech.* **212** 557-592(1990).
- [6] L. J. Bloomfield and R. C. Kerr, Turbulent fountains in a stratified fluid, *J. Fluid Mech.* **358** 335-356 (1998).
- [7] L. J. Bloomfield and R. C. Kerr, Turbulent fountains in a confined stratified environment *J. Fluid Mech.* **389** 27-54 (1999).
- [8] W.E. Lin and S. W. Armfield, Direct simulation of weak axisymmetric fountains in a homogeneous fluid, *J. Fluid Mech.* **403**, 67-88 (2000).
- [9] G. R. Hunt and N. G. Kaye, Virtual origin correction for lazy turbulent plumes, *J. Fluid Mech.* **435**, 377-396 (2001).
- [10] G. R. Hunt and N. G. Kaye, Lazy plumes, *J. Fluid Mech.* **533**, 329-338 (2005).
- [11] T. S. Richards, Q. Aubourg, and Bruce R. Sutherland, Radial intrusions from turbulent plumes in uniform stratification, *Phys. Fluids* **26**, 036602 (2014).
- [12] R. Camassa, Z. Lin, R. M. McLaughlin, K. Mertens, C. Tzou, J. Walsh and B. White, Optimal mixing of buoyant jets and plumes in stratified fluids: theory and experiments, *J. Fluid Mech.* **790** 71-103 (2016).
- [13] D. Carroll, D. A. Sutherland, E. L. Shroyer, J. D. Nash, G. A. Catania, Leigh A. Stearns, Modeling Turbulent Subglacial Meltwater Plumes: Implications for Fjord-Scale Buoyancy-Driven Circulation, *J. Phys. Oceanogr.* **45**, 2169-2185 (2015).
- [14] E. Ezhova, C. Cenedese and L. Brandt, Interaction of vertical turbulent jets with a thermocline. *J. Phys. Oceanogr.* **46**, 3415-3437 (2016).
- [15] B. R. Morton, , G. I. Taylor and J. S. Turner, Turbulent gravitational convection from maintained and instantaneous sources, *Proc. R. Soc. Lond. A* **234**, 1 (1956).
- [16] B. R. Morton, Forced plumes, *J. Fluid Mech.* **5**, 151-163, (1959).
- [17] B. R. Morton and J. Middleton, Scale diagrams for forced plumes. *J. Fluid Mech.* **58**, 165-176 (1973).
- [18] L. J. Bloomfield and R. C. Kerr, A theoretical model of a turbulent fountain, *J. Fluid Mech.* , **424**, 197-216 (2000).
- [19] T. J. McDougall, Negatively buoyant vertical jets, *Tellus* **33**, 313-320 (1981).
- [20] E. Kaminski, S. Tait and G. Carazzo, Turbulent entrainment in jets with arbitrary buoyancy, *J. Fluid Mech.* **526**, 361-376 (2005).
- [21] G. Carazzo, E. Kaminski and S. Tait, The rise and fall of turbulent fountains: A new model for improved quantitative predictions, *J. Fluid Mech.*, **657**, 265-284 (2010).
- [22] R. Mehaddi, O. Vauquelin and F. Candelier, Analytical solutions for turbulent Boussinesq fountains in a linearly stratified environment, *J. Fluid Mech.* **691**, pp. 487-497 (2012).
- [23] J. S. Turner, *Buoyancy Effects in Fluids* (Cambridge University Press, 1973).
- [24] P. Papanicolaou and G. Stamoulis, Spreading of buoyant jets and fountains in a calm, linearly density-stratified fluid, *Proc., 6th Int. Symp. on Environmental Hydraulics*, Taylor & Francis, London (2010).
- [25] J. W. Telford 1966 The convective mechanism in clear air. *J. Atmos. Sci.* **23**, 652-666 (1966).
- [26] M. van Reeuwijk and J. Craske, *J. Fluid Mech.* **782** 333-355 (2015).
- [27] D. Freire, C. Cabeza, S. Pauletti, G. Sarasua, I. Bove, G. Usera, A. C. Marti, Effect of turbulent fluctuations on the behaviour of fountains in stratified environments, *J. Phys.: Conf. Ser.* **246** 012015 (2010).
- [28] D. Freire, S. Kahan, C. Cabeza, G. Sarasua, and A. C. Marti, The formation of coherent structures within turbulent fountains in stratified media, *European Journal of Mechanics-B/Fluids* **50** 89-97 (2015).
- [29] Fischer, H.B., List, E.J., Koh, R.C.Y., Imberger, J. & Brooks, N.H. 1979. *Mixing in inland and coastal waters*, Academic Press.
- [30] Wood, I. R., Bell, R.G. Wilkinson, D.R. 1993. *Ocean Disposal of wastewater*. Adv. Series on Ocean Eng. Vol. 8, World Scientific.
- [31] J. H. W. Lee and V. H. Chu, *Turbulent jets and plumes - a lagrangian approach*, Kluwer academic publishers (2003).
- [32] G. Usera, A. Vernet, and J.A. Ferre, A parallel block-structured finite volume method for flows in complex geometry with sliding interfaces, *Flow, Turbulence and Combustion*, 81 **3** 471, (2008).
- [33] M. Mendina, M. Draper, A. P. Kelm Soares, G. Narancio, and G. Usera, A general purpose parallel block structured open source incompressible flow solver, *Cluster Computing*, 17 **2** 231-241 (2014).